Kinetic Properties of the Acceptor Quinone Complex in *Rhodopseudomonas viridis*

Winfried Leibl*,‡ and Jacques Breton

Section de Bioénergétique, Département de Biologie Cellulaire et Moléculaire, CEN Saclay, 91191 Gif-sur-Yvette Cedex, France

Received April 24, 1991; Revised Manuscript Received June 26, 1991

ABSTRACT: The kinetics of electron transfer from the primary (Q_A) to the secondary (Q_B) quinone acceptor in whole cells and chromatophores of *Rhodopseudomonas viridis* was studied as a function of the redox state of Q_B and of pH by using a photovoltage technique. Under conditions where Q_B was oxidized, the reoxidation of Q_A^- was found to be essentially monophasic and independent of pH with a half-time of about 20 μs. When Q_B was reduced to the semiquinone form by a preflash, the reoxidation of Q_A^- was slowed down showing a half-time between 40 and 80 μs at pH $\leq$ 9. Above pH 9, the rate of the second electron transfer decreased nearly one order of magnitude per pH unit. After a further preflash, the fast and pH-independent kinetics of Q_A^- reoxidation was essentially restored. The concentration of Q_A still reduced 100 μs after its complete reduction by a flash showed distinct binary oscillations as a function of the number of preflashes, confirming the interpretation that the electron-transfer rate depends on the redox state of Q_B. After addition of *o*-phenanthroline, the reoxidation of Q_A^- is slowed down to the time range of seconds as expected for a back-reaction with oxidized cytochrome. Under conditions where inhibitors of the electron transfer between the quinones fail to block this reaction in a fraction of the reaction centers due to the presence of the extremely stable and strongly bound semiquinone, Q_B^-, these reaction centers show a slow electron transfer on the first flash and a fast one on the second, i.e., an out-of-phase oscillation. The decrease of the electron-transfer rate on the second flash and the effect of pH are discussed with respect to the influence of the protein surrounding.

The primary reactions in the reaction center (RC)[1] of photosynthetic purple bacteria were intensively studied. Together with the now available structural information, these studies led to a considerable understanding of the structure–function relationship in these transmembrane protein complexes that are often considered as a model for the whole variety of photosynthetic RC [for a review, see Feher et al. (1989) and Huber (1989)]. The prosthetic groups bound to the heterodimeric core polypeptides called L and M are four bacteriochlorophylls, two bacteriopheophytins, two quinones, and one non-heme iron. After excitation of the primary donor (P), a special pair of bacteriochlorophylls, charge separation takes place, and an electron is transferred along one of two symmetric branches that is built by a bacteriochlorophyll, a bacteriopheophytin (BPhe) and a quinone (Q_A), thereby crossing the membrane. In isolated RC the primary radical pair P^+BPhe^- is formed in about 3 ps, and the electron is stabilized on the first quinone acceptor, Q_A, in about 200 ps if Q_A is oxidized. When Q_A is reduced before light excitation, the primary radical pair decays in the nanosecond time range by several paths including back-reaction either to the ground state or the excited state of singlet or triplet character. Secondary electron transfer includes the reoxidation of Q_A^- by electron transfer to the secondary quinone acceptor, Q_B, and the rereduction of P^+ by secondary donors. In the case of *Rhodopseudomonas viridis* a tightly bound tetraheme cytochrome subunit can rereduce P^+ in the submicrosecond range (Holten et al., 1978).

In this work we shall focus on the reactions on the acceptor side [for a review, see Crofts and Wraight (1983)]. In *Rps. viridis*, Q_A is menaquinone and Q_B is ubiquinone. But even when both are the same chemical species, as for example in *Rhodobacter sphaeroides*, their function in electron transfer in the RC is different. Q_A is tightly bound to the protein and under physiological conditions accepts only one electron. Q_B is weakly bound, except in the singly reduced semiquinone state (Diner et al., 1984). It accepts consecutively two electrons from Q_A together with the uptake of two protons. The quinol formed can leave the RC and be replaced by a quinone from the pool of quinones in the membrane (McPherson et al., 1990). Thus the quinone–iron acceptor complex works as a two-electron gate, which leads to the well-established binary oscillation behavior between the quinone and semiquinone form of Q_B in successive flashes (Vermeglio, 1977; Vermeglio & Clayton, 1977; Wraight, 1977). Information obtained from the three-dimensional structure of the RC supports the idea that the different local protein environment is responsible for the different function of the quinones, and much effort has been made (especially by site-specific mutagenesis) to obtain a more detailed picture of the molecular mechanism underlying the function.

Equilibrium redox titrations show a pH dependence of the midpoint potential (E_m) of Q_A (–60 mV/pH) up to a pK of about 7.8 in *Rps. viridis* (Prince et al., 1976). Q_A^- is not protonated directly during photosynthetic electron transfer, the protonation rather involving the protein, as proposed recently for *Rb. sphaeroides* (Maroti & Wraight, 1988; McPherson et al., 1988). Probably a shift in the pK values of several protonatable amino acid residues induced by the electrical charge on Q_A leads to a partial proton uptake. The

* To whom correspondence should be addressed.

‡ W.L. was supported by the Deutsche Forschungsgemeinschaft (DFG).

[1] Abbreviations: RC, reaction center(s); P, primary electron donor; BPhe, bacteriopheophytin; Q_A and Q_B, primary and secondary quinone acceptor; DAD, diaminodurene (2,3,5,6-tetramethyl-*p*-phenylenediamine); TMPD, *N,N,N',N'*-tetramethyl-*p*-phenylenediamine; CCCP, carbonyl cyanide *m*-chlorophenylhydrazone

0006-2960/91/0430-9634$02.50/0

protonation state of nearby amino acid residues, on the other hand, influences the redox midpoint potential of the quinone. In *Rb. sphaeroides* it was shown that an even stronger interaction with protonatable groups exists in the case of Q_B and the resulting change in free energy between the states $Q_A^-Q_B$ and $Q_AQ_B^-$ contributes to the driving force for the electron transfer between the quinones (Kleinfeld et al., 1984). For the first reduction of Q_B the protonation of the RC serves to stabilize the semiquinone that is not protonated directly, whereas the formation of the quinol after a second charge separation implies that two protons must be supplied to Q_B before it can leave the RC and be replaced by an oxidized quinone. These protons that are taken up in the RC at the cytoplasmic side of the membrane and released into the periplasmic compartment during the oxidation of the quinol by the cytochrome b–c_1 complex are the main contribution to the transmembrane proton gradient that drives the synthesis of ATP and plays a crucial role in photosynthetic energy conversion.

The Q_B site is of interest also from another point of view: it constitutes the site of action of many herbicides that compete with Q_B at its binding site and block secondary electron transfer. The efficiency of different inhibitors seems to be governed by the same mechanisms that determine the properties of the two quinone acceptors, namely, their interaction with amino acid residues in the binding pocket. Therefore the study of well-characterized herbicide-resistant mutants can give useful information on the structure–function relationship of electron and proton transfer on the acceptor side of photosynthetic RC.

The interquinone electron transfer in purple bacterial RC has been studied by different methods. The most direct method is the detection of absorbance changes related to the redox state of Q_A or Q_B, either direct quinone absorption bands or electrochromic shifts of the BPhe absorption, that are different for the two anionic semiquinones, Q_A^- and Q_B^-, especially in the near-infrared region (Verméglio & Clayton, 1977; Verméglio, 1982; Shopes & Wraight, 1985). However, complications of these measurements by possible contributions of other absorbance changes and the necessary high time resolution have so far hindered its use for kinetic measurements in *Rps. viridis*.

Other more indirect methods are double-flash measurements. The yield of cytochrome oxidation on the second flash in *Rps. viridis* was measured by Carithers and Parson (1975). They reported half-times for Q_A^- reoxidation varying from 6 to 30 μs between pH 7 and 8. Beside this early work and some recent results obtained by measuring the long-lived (>millisecond) formation of P^+ in the near-infrared (Mathis, personal communication), to our knowledge there are no other kinetic data available. Thus, in contrast to the situation in *Rb. sphaeroides* where the kinetics of the electron transfer between the quinones are well studied and detailed energetic models have been proposed, in *Rps. viridis* information about these reactions is still sparse.

Time-resolved photovoltage measurements have already been used to study the primary electrogenic reactions in whole cells of *Rps. viridis* and *Rb. sphaeroides* (Deprez et al., 1986, Dobek et al., 1990, Trissl et al., 1990). They allowed direct measurements of the transmembrane electron transfer from P to BPhe and then to Q_A and the evaluation of the relative dielectrically weighted distances between the electron carriers. The electron transfer from Q_A to Q_B is not electrogenic (Dracheva et al., 1988) and can therefore not directly be observed by a photovoltage technique. However, in a double-flash experiment the reoxidation of the primary quinone acceptor can be followed. Whereas with oxidized Q_A the photovoltage signal is composed of the primary charge separation step of BPhe reduction and the subsequent electron transfer to Q_A, this latter positive phase is replaced by a negative phase due to the back-reaction of the primary radical pair if Q_A is already (or still) reduced.

In this study we used the sensitivity of the photovoltage kinetics to the redox state of Q_A to study by double-flash measurements the reoxidation of this component in the intact system. By choosing appropriate redox conditions and by varying the number of preflashes prior to the probe flash, the kinetics of electron transfer from Q_A to the oxidized and semireduced form of Q_B were studied as a function of pH. We show that the interquinone electron transfer is quite fast and independent of pH if Q_B is oxidized. However, if the latter is already semireduced, its further reduction is slowed down and becomes proportional to the bulk proton concentration above a pH of about 9.4, indicating that a concomitant proton uptake might be the rate-limiting step for the transfer of the second electron.

Experimental Procedures

Cultures of *Rps. viridis* cells were grown as described (Cohen-Bazire et al., 1957). Chromatophores were prepared from the cells by a French press treatment followed by sucrose density gradient centrifugation. Samples were stored as a pellet at −30 °C until use. For measurements, they were thawed, diluted in 10 volumes of 50 mM buffer, and incubated about 5 min with 5 mM ferricyanide and 200 μM DAD before being washed two times in 10 volumes of 50 mM buffer. The following buffers were used: MOPS (pH 7), tricine (pH 8), and glycine (pH 9–11). For whole cells about 2 μg/mL of gramicidin and of the uncoupler CCCP were present from the first washing step on to ensure pH equilibration and to shunt the membrane potential. The pH was checked in the last supernatant. Chromatophores were washed in 10 mM buffer to decrease the salt concentration as necessary for electrical orientation. Redox chemicals and inhibitors were added before the measurement as indicated. With whole cells, the photovoltage kinetics were measured according to the light-gradient technique essentially as described earlier (Trissl et al., 1987b). Chromatophores were oriented by sedimentation on the platinum electrode of the microcoaxial measuring cell by applying a short electric field pulse (ca. 500 V/cm, 100 ms). The concentration of the samples corresponded to an optical density at 532 nm of about 0.5 (d = 0.01 cm). Submicrosecond preflashes were obtained from a dye laser (Electro-Photonics Ltd., model 23) operated with rhodamine 6G (600 nm, ≈ 10 mJ/cm², FWHM 200 ns). The picosecond probe flash was from a mode locked, frequency doubled Nd-YAG laser (Quantel, France, FWHM 30 ps), the energy of which was attenuated by neutral density filters to about 250 μJ/cm² in order to be in the quasilinear range of the saturation curve. This excludes complications by nonlinear effects of the light gradient (Leibl & Trissl, 1990). It was checked that the preflashes were saturating and the energy was stable from flash to flash for a spacing of 100 ms between multiple preflashes. The delay between the (last) preflash and the picosecond probe flash was monitored with an oscilloscope. Due to the jitter inherent to the picosecond flash, for delay times shorter than about 30 μs the shots were selected into separate groups to average only data with an identical delay within the error of 5% or 1 μs, whatever is larger. In general, between 5 and 10 traces were averaged with a spacing of not less than 10 s between each cycle. After about 30 shots, the sample was

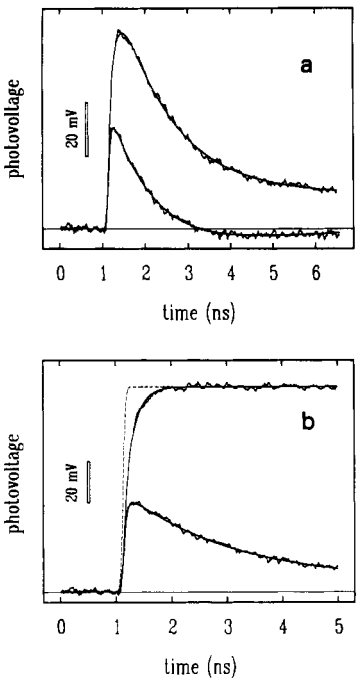

FIGURE 1: (a) Kinetics of the photovoltage in whole cells of *Rps. viridis* evoked by a picosecond laser flash (30 ps FWHM) determined in 10 mM DAD, 10 mM *o*-phenanthroline, and 50 mM glycine, pH 9.0. The excitation energy was ca. 250 $\mu J/cm^2$. The data correspond to an average of 10 (upper trace) and 7 (lower trace) traces. The smooth lines are best fits according to the reaction scheme described in the text. The time constants used are $\tau_1 = 25$ ps, $\tau_2 = 175$ ps, $\tau_3 = 40$ ps, and $\tau_4 = 2$ ns. The relative electrogenicity factors used are $A_1 = A_3 = 1$, $A_2 = 1.2$, $A_4 = -1$. (Upper trace) without preflash; (lower trace) with a saturating preflash given 20 μs before the picosecond flash. In the lower trace the kinetics were decomposed (see Results) into 96% kinetics (2) and 4% kinetics (1) yielding 96% of Q_A reduced. (b) The same data as in panel a with the instrumental capacitative decay ($\tau \approx 1.3$ ns) deconvolved. (Dashed line) Best fit of the deconvolved photovoltage kinetics from oriented purple membranes (*Halobacterium halobium*), demonstrating the time resolution of the apparatus.

changed. For every sample, at the beginning and the end of data acquisition, reference kinetics without preflash were recorded to calibrate the photovoltage kinetics for fully oxidized primary acceptor and to detect any alteration of the sample during the measurement. Analysis of the kinetics was performed by iterative convolution of a linear combination of the charge separation kinetics in the case of oxidized and reduced Q_A with the apparatus response function as described elsewhere (Trissl et al., 1987a). The determined values for the fraction of reduced Q_A at different delay times between preflash and probe flash were subjected to a nonlinear least-squares fit procedure (Leatherbarrow, 1989) to extract the kinetics of the Q_A^- decay.

RESULTS

Basic Photovoltage Kinetics. The observed kinetics of the photovoltage in whole cells of *Rps. viridis* with Q_A oxidized and Q_A largely reduced are shown in Figure 1a (upper and lower trace, respectively). In both experiments, 10 mM *o*-phenanthroline was present and in the lower trace a saturating preflash was given 20 μs before the picosecond flash. The overall shape of the traces is largely determined by the discharge of the capacitative measuring cell that leads to a differentiation of the photovoltage signal with a time constant of about 1.3 ns. To reveal the pertinent information, it is useful to display the kinetics after deconvolution of the capacitative discharge (identical for both traces) as shown in Figure 1b. In this form the amplitudes and kinetics can directly be assigned to the electron transfer steps in the RC. The difference between the two traces with and without preflash is due to the replacement of the ≈200 ps rise of electrogenicity according to electron transfer from BPhe to Q_A by a 2-ns back-reaction of the primary radical pair (Trissl et al., 1990). The photovoltage kinetics were virtually identical when Q_A was prereduced either by background light in the presence of the inhibitor *o*-phenanthroline or chemically by the addition of dithionite. Under the latter conditions, strong white background light led to the disappearance of the signal as a result of accumulation of reduced BPhe (Deprez et al., 1986). The kinetics were essentially the same in whole cells and chromatophores (data not shown). In the case of reduced Q_A, the maximum amplitude of the photovoltage before deconvolution was decreased to about 50%.

The kinetics of the charge separation can be described by the following reaction scheme:

RC with Q_A oxidized

$$P\,BPhe\ Q_A \xrightarrow[A_1]{\tau_1} P^+BPhe^-\ Q_A \xrightarrow[A_2]{\tau_2} P^+BPhe\ Q_A^- \quad (1)$$

RC with Q_A reduced

$$P\,BPhe\ Q_A^- \xrightarrow[A_3]{\tau_3} P^+BPhe^-\ Q_A^- \xrightarrow[A_4]{\tau_4} P\,BPhe\ Q_A^- \quad (2)$$

The kinetics in the case of oxidized Q_A are determined by three parameters, the trapping time τ_1, defined as the time constant of the appearance of the first charge-separated state (P^+BPhe^-), the time constant for the second step of charge separation (Q_A reduction) τ_2, and the electrogenicity of this electron transfer step relative to the first one, A_2/A_1. Similarly, in the case of reduced Q_A the trapping time τ_3, the time constant for the back-reaction τ_4, and the relative electrogenicity of the back-reaction A_4/A_3 are involved.

From Figure 1, it can be seen that, once the parameters of the photovoltage kinetics in the extreme cases of completely oxidized and reduced RC are determined, an analysis of the photovoltage kinetics allows for the extraction of the fraction of Q_A reduced at the moment the picosecond probe flash was given. This determination can be done by a fit of the photovoltage kinetics optimizing one single parameter. The dependence of the fraction of RC with Q_A still reduced as a function of the corresponding delay time between preflash and probe flash gives the kinetics of Q_A^- reoxidation under the reasonable assumption that the transfer of an electron from BPhe to Q_A is only possible if Q_A is oxidized.

The yield of the first step of charge separation is independent of the redox state of Q_A in *Rps. viridis* (Trissl et al., 1990). Therefore, in our case it is essentially the time constants and relative amplitudes of the second steps in the reaction schemes 1 and 2 that are important.

The relative amplitude of the back-reaction is usually taken as −1. This and the simple scheme 2 imply that the back-reaction is monophasic. The high signal-to-noise ratio of the present measurements, especially with oriented membranes, showed that this is not exactly true: the fit of the decay of the primary radical pair in the presence of reduced Q_A by a single exponential showed significant deviations that could be accounted for by assuming that about 10–15% of the radical pair decays more slowly than the dominant part. The reason for this could be a heterogeneity of charge recombination, perhaps due to a relaxation of the radical pair (Sebban & Barbet, 1984; Woodbury & Parson, 1984) or other than exponential kinetics, perhaps connected to a partial formation

and decay of the radical pair triplet state. A detailed study of the back-reaction, however, is beyond the scope of this work and will be treated in another publication. We used for the analysis a single-exponential decay with a time constant of 2 ns. It was checked that fitting the decay of the primary radical pair by a single or double exponential had only a minor effect (less than 2%) on the evaluation of the fraction of reduced RC, which is investigated in the present study.

In the case of oxidized Q_A, there is an uncertainty inherent in the analysis concerning the value of the relative electrogenicity of the second electron-transfer step (parameter A_2 in Figure 1). This value cannot be extracted with reasonable precision from a kinetic analysis alone. Therefore, in an earlier publication this parameter was determined by using multiple information (Trissl et al., 1990). We now have indications that the kinetics and/or electrogenicity of this phase depend somewhat on the preparation and the ionic conditions. However, the value of the electrogenicity of Q_A reduction affects mainly the amplitude and hardly the kinetics of the photovoltage. Because the analysis presented here is based on the kinetics rather than on the amplitude of the photovoltage, the uncertainty in the value of A_2 is not critical. The close agreement between the concentration of reduced Q_A extracted from the analysis of either the kinetics or the maximum photovoltage amplitude (not shown) confirmed the value of $A_2 \approx 1.2$ used for the analysis. The other values of the parameters that describe the photovoltage kinetics in the case of oxidized and reduced Q_A and that are used for the evaluation of the fraction of RC with Q_A reduced are given in Figure 1.

Reoxidation Kinetics of Q_A^-. By varying the delay time between a saturating preflash and the picosecond probe flash, we studied the reoxidation kinetics of Q_A^- created by the preflash at various pH. In addition, to detect any change in the electron-transfer rate to either Q_B or Q_B^-, we varied the number of preflashes to switch the RC between these states. For this experiment to work, it was necessary to add an appropriate redox mediator in a concentration high enough to reoxidize any Q_B^- in the dark time between the averaging cycles (about 10 s) but not within the time between two preflashes (100 ms). We found that under our conditions this could reasonably be achieved by the addition of 10 mM DAD or of 1–3 mM TMPD (see Discussion). To prove that the reoxidation of Q_A^- is really due to the electron transfer to Q_B and not to some external acceptor, we measured, as a control the same process, the reoxidation of Q_A^- after addition of the inhibitor *o*-phenanthroline, which is known to block electron transfer beyond Q_A (Verméglio et al., 1980).

The fraction of reduced Q_A as a function of (delay) time after one and two saturating preflashes is shown in Figure 2 on a logarithmic time scale for the lowest and highest pH value studied in the presence of 10 mM DAD and 3 mM TMPD, respectively. For a satisfying fit of the Q_A^- reoxidation kinetics, generally neither a single-exponential (first-order reaction) nor a single-hyperbolic kinetics (second-order reaction) was sufficient. With two-exponential phases, however, the data could be well described, the resulting kinetics lying somewhere between the two simple cases stated above. When the rates differed by less than a factor of about 5, the data did not allow the extraction of the parameters of this biexponential kinetics with reasonable precision. In this case, the half-times are used to describe the kinetics.

The reoxidation of Q_A^- after a single saturating preflash (open circles in Figure 2) displayed a half-time of about 20 μs both at pH 7 (Figure 2a) and pH 11 (Figure 2b). The open

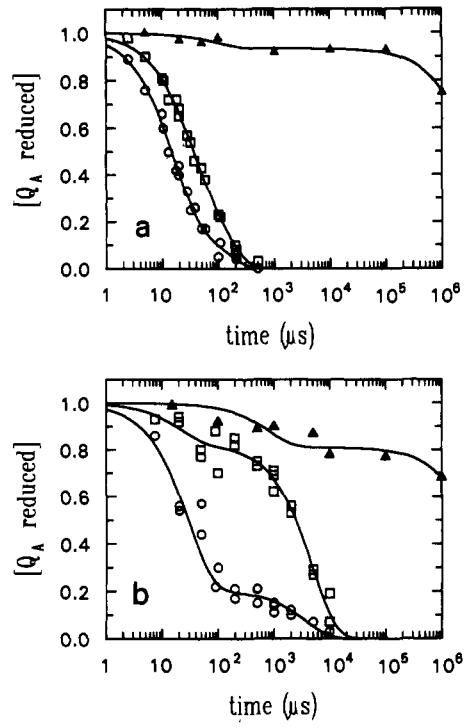

FIGURE 2: Decay kinetics of Q_A^- after one (○) and two (□) saturating preflashes. Shown are data from two sets of experiments. Solid lines show the best fit of two exponentials. (▲) Same conditions as for (○) but in the presence of 10 mM *o*-phenanthroline. (a) pH 7, DAD (10 mM) added. (b) pH 11, TMPD (3 mM) added.

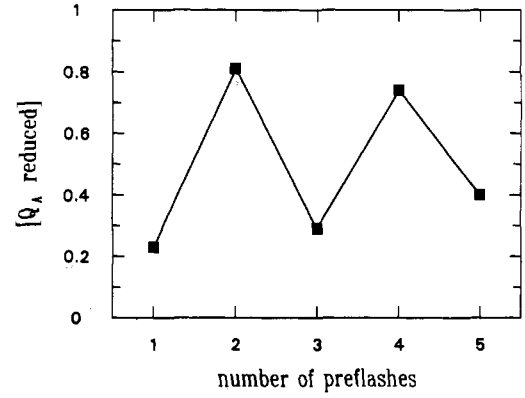

FIGURE 3: Binary oscillation of Q_A^- reoxidation rate. The fraction of Q_A still reduced 100 μs after the last preflash as a function of the number of preflashes is shown. Preflashes were spaced 100 ms apart. DAD (10 mM) was added, pH 10. Other experimental conditions were as given in the legend to Figure 2.

squares in Figure 2 show the same experiment as the open circles with the same sample except that an additional preflash was given 100 ms before. Under these conditions, the reoxidation kinetics of Q_A^- were slowed down about 2-fold at pH 7. At higher pH the effect was much more pronounced, the deceleration reaching a factor of >100 at pH 11 (Figure 2b). At all pH values a third preflash had the effect to bring the Q_A^- reoxidation kinetics back very close to the one after only one preflash although a small fraction of the slower kinetics remained (data not shown). At high pH (Figure 2b) there is obviously a 20% phase with the "wrong" kinetics present (slow on the first preflash, fast on the second preflash). As we will discuss below, this phase can be attributed to a residual fraction of Q_B^- present before the flash sequences. In Figure 3 it is shown that when the fraction of Q_A still reduced after 100 μs is plotted against the number of preflashes (spaced 100 ms) a damped binary oscillation is found. This means that

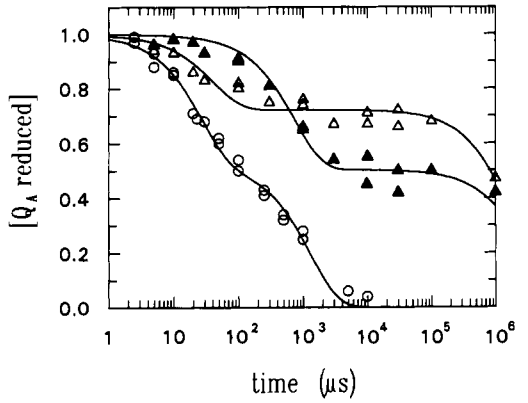

FIGURE 4: Decay kinetics of Q_A^-. 500 μM DAD was added, pH 10. (○) No *o*-phenanthroline, one preflash; (▲) 10 mM *o*-phenanthroline, one preflash; (△) 10 mM *o*-phenanthroline, two preflashes spaced 100 ms apart. Data from two sets of experiments are shown.

the electron transfer from Q_A to the next electron carrier is faster on odd-numbered preflashes and slower on even-numbered preflashes, a behavior that can be attributed to Q_B functioning as a two-electron gate. Although this oscillation is present at all pH values, it is more pronounced at high pH, where the difference between the first and second electron transfer rate is much larger (compare panels a and b in Figure 2).

To corroborate the assignment of the observed Q_A reoxidation to the electron transfer to Q_B, control measurements were made after addition of the inhibitor *o*-phenanthroline to the sample. Neither a significant decrease of the photovoltage amplitude nor a change of the photovoltage kinetics induced in dark-adapted samples was found upon addition of the inhibitor. The effect of the addition of 10 mM *o*-phenanthroline on the decay of Q_A^- is also shown in Figure 2 (triangles). More than 90% of the RC at pH 7 and about 80% at pH 11 showed a slow reoxidation of Q_A^- in the second range that is expected for a back-reaction with oxidized cytochrome (Shopes & Wraight, 1985; Gao et al., 1990).[2] Carithers and Parson (1975) reported that blocking of the electron transfer by *o*-phenanthroline is not complete but saturates at about 88% blockage. This could explain why we never succeeded in blocking 100% of the RC by *o*-phenanthroline, as obvious from the ≈10% rapid reoxidation of Q_A^- found in our experiments (see Figure 2a). The larger fraction of RC not blocked at high pH (Figure 2b) is most likely caused by a residual fraction of Q_B^- in the dark (see below and Discussion).

The different Q_A^- reoxidation kinetics after one and two preflashes (Figure 2) and the oscillation behavior obvious in Figure 3 were seen only in the presence of a relatively high concentration of DAD (10 mM) or TMPD (1–3 mM; we suppose that the high concentration necessary to oxidize Q_B^- is due to the fact that under our experimental conditions the mediators were largely reduced). If only 500 μM DAD was added, no significant oscillation was observed and the reoxidation kinetics of Q_A^- were the same after one and two preflashes (data not shown). However, the Q_A^- reoxidation kinetics were clearly biphasic, and they could at all pH be well fitted by about equal amounts of the fast and the slow kinetics after one and two preflashes described above (Figure 2). This behavior is shown in Figure 4 (circles) for high pH (10) where the two phases are well separated.

[2] Q_A^- has not decayed completely after the longest delay time in Figure 2 (1 s) but has decayed almost completely within the time between the averaging cycles (10 s).

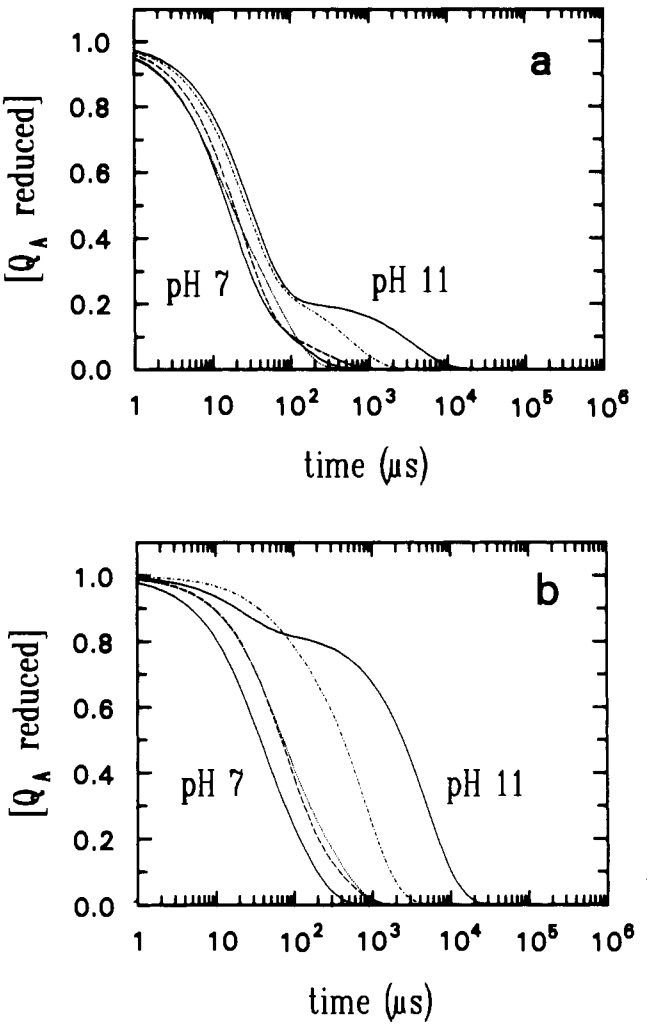

FIGURE 5: Best fits (two exponentials) of the reoxidation kinetics of Q_A^- measured in the presence of 10 mM DAD (pH 7–10) or 1–3 mM TMPD (pH 10 and 11) at different pH. (a) Following the first preflash; (b) following the second preflash. (Solid lines) left, pH 7; right, pH 11; (dashed line) pH 8; (dotted line) pH 9; (dashed-dotted line) pH 10. For the minor phase at pH 10 and 11, see the text.

The effect of *o*-phenanthroline under this condition was very incomplete. Only 50% of Q_A^- decays by back-reaction (Figure 4, filled triangles). Moreover, the decay of Q_A^- in the RC that are not blocked by the inhibitor was clearly identical with the slower phase found in the absence of the inhibitor, whereas an additional preflash restored partly the faster phase (compare open and closed triangles in Figure 4). This means the RC that are not blocked show an out-of-phase oscillation. Together with the Q_A^- reoxidation kinetics in the absence of *o*-phenanthroline, these findings indicate that prior to the flash sequence about 50% of the RC were in the state Q_B^-, a state that is known to prevent the binding of *o*-phenanthroline (Verméglio et al., 1980; Wraight & Stein, 1980). A more complete blocking could neither be achieved by an increase of the concentration nor by a change of the nature of the inhibitor (terbutryn at 100 μM) but was reached by a further addition of DAD or TMPD. In part this out-of-phase oscillation is also well seen in Figure 2b at high pH for a minor 20% fraction showing a slow electron transfer on the first flash and a fast one on the second flash. This would also explain the less efficient blocking by *o*-phenanthroline under these conditions (Figure 2b) compared to normal pH (Figure 2a).

For an easier comparison, the electron transfer kinetics on the first and second preflash measured for a pH varying be-

Table I: Half-Times of the Electron Transfer Kinetics from Q_A^- to Q_B and Q_B^-

	pH				
	7	8	9	10	11
$Q_A^- \rightarrow Q_B$	17 ± 3 μs	19 ± 3 μs	18 ± 4 μs	19 ± 3 μs	21 ± 3 μs
$Q_A^- \rightarrow Q_B^-$	40 ± 10 μs	10 ± 15 μs	80 ± 25 μs	540 ± 50 μs	3.3 ± 0.3 ms

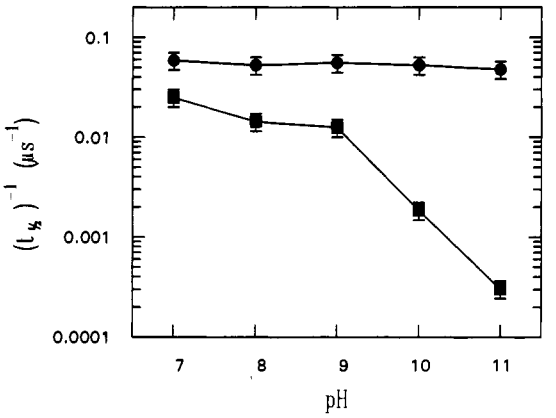

FIGURE 6: Rate of Q_A^- reoxidation as a function of pH for the states Q_B (●) and Q_B^- (■). Rate constants were calculated as $(\tau_{1/2})^{-1}$. Error bars show cumulative errors due to different sets of experiments and the standard deviation of the parameters of the kinetic analysis.

tween 7 and 11 is shown in Figure 5, panels a and b, respectively. The corresponding half-times are listed in Table I together with the estimated error that takes into account variations between different experiments and the standard deviation of the kinetic analysis. As a basis for an interpretation in terms of energetics, a half-logarithmic plot of rate constants as a function of pH is commonly used. Such a plot of rate constants calculated as the reciprocal of the half-times is shown in Figure 6. It can be seen that the rate of the first electron transfer stays rather constant over the whole pH range studied. In contrast, for the second electron transfer, a range of only slight pH dependence at low pH changes above pH 9 into a region where the rate decreases linearly with the proton concentration.

Discussion

Redox State of Q_B. Continuous illumination leads to an equilibrium concentration of 50% of Q_B in the semiquinone form even if the intensity is very weak. This is a consequence of the much stronger (10^5) binding of this form compared to Q_B and Q_BH_2 (Crofts & Wraight, 1983). One photon per RC within the lifetime of the semiquinone is sufficient to keep 50% of Q_B in the semiquinone form. On the other hand, it is not possible to increase the concentration of Q_B^- to above 50% by increasing the intensity of the continuous light because under this condition for every RC where Q_B^- is created after the absorption of a photon, there is another one where at the same time Q_B becomes doubly reduced and replaced by an oxidized quinone if available from the pool. The extent and kinetics of the reoxidation of the semiquinone depend strongly on the redox potential and the presence of a suitable mediator (Mulkidjanyan et al., 1986). Whereas in isolated RC the acceptor side is accessible for artificial acceptors such as ferricyanide (Shopes & Wraight, 1986) that might reoxidize Q_B via Q_A, in chromatophores or even whole cells the semiquinone can be extremely stable.

In our experiments it turned out that the deceleration of the Q_A^- reoxidation by inhibitors like *o*-phenanthroline is a very precise monitor of the presence of Q_B^-, a state in which inhibition of electron transfer fails. Without a sufficient amount of redox mediators like DAD or TMPD, even prolonged dark adaptation under our aerobic conditions did not lead to a complete reoxidation of this electron carrier. Interestingly, at low pH in the absence of DAD or TMPD, the addition of *o*-phenanthroline led to a significant reduction of Q_A in the dark. This effect disappeared at higher pH (10) and can be attributed to the p*K* shift of Q_A from 7.8 to 10 induced by *o*-phenanthroline (Prince et al., 1976). This observation shows at the same time that the pH adjusted in the external phase of the cell suspension was operative also on the cytoplasmic side of the photosynthetic membrane, a prerequisite for the study of pH effects on acceptor side reactions.

To study the influence of the redox state of Q_B on the electron transfer, it is desirable to prepare the semiquinone state in all RC. Because of the overlapping redox transitions between Q_B/Q_B^- and Q_B^-/Q_BH_2 this cannot be achieved by redox titration, at least not at normal pH (Rutherford et al., 1979; Rutherford & Evans, 1979). A possibility is to convert all RC from the state Q_B to Q_B^- by a saturating preflash, but this requires that all RC are in the state Q_B before the preflash. When we optimized the concentration of the redox mediator, it turned out that at the concentration necessary to completely oxidize Q_B^- in the dark or in the 10 s interval between the flash groups (monitored by the effect of *o*-phenanthroline or by the almost complete removal of the slow phase on the first preflash at high pH; see Figure 2b and 4), a significant fraction of Q_B^- created by the first preflash was already reoxidized during the 100 ms delay before the second preflash. This apparent contradiction could be explained by a heterogeneous Q_B^- reoxidation that is severely hindered in about 20% of the RC. One might speculate that this fraction of RC could also be responsible for the damping of the oscillation (Figure 3) and the incomplete regeneration of the fast Q_A^- reoxidation phase in the two-preflash experiment of Figure 4 (open triangles). In these RC the exchange of Q_BH_2 by oxidized Q_B within the 100 ms between the preflashes could fail perhaps due to the redox state of the quinone pool.

Another possible explanation for the incomplete fast reoxidation of Q_A^- on the first preflash at high pH (Figure 2b) could be based on an analogy to the situation in other purple bacteria. In *Rb. sphaeroides* as well as in *Chloroflexus aurantiacus* the one-electron transfer equilibrium between $Q_A^-Q_B$ and $Q_AQ_B^-$ was found to approach 1 at high pH, i.e., the state $Q_A^-Q_B$ becomes energetically more favored at high pH (Kleinfeld et al., 1984; Venturoli & Zannoni, 1988). We can reject this possibility for two reasons. First, in *Rps. viridis* the apparent equilibrium constant was found to be considerably higher than in *Rb. sphaeroides* and relatively constant between pH 7 and 11 (Wraight et al., 1987; Baciou et al., 1990; Gao et al., 1991). Second, the fraction of Q_A^- where electron transfer to Q_B fails should be stable for at least the lifetime of Q_B^- (>100 ms) and decay either by back-reaction or electron transfer to external acceptors. The minor slow phase, however, shows a reoxidation of Q_A^- in some milliseconds that can hardly be explained by a one-electron transfer equilibrium shifted in favor of the state $Q_A^-Q_B$. Thus the data show that in *Rps. viridis* electron transfer to Q_B is largely energetically favored even at pH 11.

It should be noted that for pH >10 the redox mediator DAD was no longer capable of completely oxidizing Q_B. This is the

consequence of the proton uptake by DAD upon reduction over the whole pH range, which leads to a roughly −60 mV/pH unit dependence of the redox midpoint potential on pH, reaching 0 mV at about pH 11 (Prince et al., 1981). At high pH, we therefore used the chemically similar TMPD that shows a pH-independent redox midpoint potential above its pK of about 6.5 (Prince et al., 1981). In fact, TMPD was found to be more efficient at high pH than DAD, but the equilibration across the membrane seemed to be more difficult in the case of TMPD. In addition, we found that TMPD at concentrations higher than a few millimolar diminished considerably the photovoltage amplitude induced by the nonsaturating picosecond flash. Guided by the fact that the relationship between the amplitude and the concentration of TMPD followed a typical Stern–Volmer plot (data not shown), we tentatively attribute this effect to a quenching of excited states in the antenna that affects the trapping yield. Therefore, we used TMPD only at high pH.

Summing up, we propose that the minor phase in the Q_A^- reoxidation kinetics at high pH (Figures 2b and 5) is not due to a biphasic electron transfer kinetics but is rather the result of a residual fraction of Q_B not being in the same redox state as the bulk population. This conclusion is mainly based on the observation that this minor phase shows out-of-phase binary oscillations and is affected by the concentration of redox mediators.

Kinetics of the First Electron Tranfer, $Q_A^- \rightarrow Q_B$. For a single Q_A^- reoxidation kinetics, the analysis of the data gives no clear indication for or against the use of a first-order kinetics to describe the decay. This is mainly due to the noise that is present in the data, especially in the tail where the concentration of Q_A^- approaches zero. However, the analysis of a large number of such kinetics shows rather clearly that they cannot simply be described by a single first-order reaction. We found that under conditions where both redox states of Q_B were present (low concentration of DAD) and the kinetics of the first and second electron transfer were not well separated (pH $\leq$9) the Q_A^- reoxidation kinetics could be described by a single second-order kinetics.

It has already been suggested that electron transfer between the quinones in purple bacteria follows a kinetics that is somewhere between first and second order (Parson, 1969; Carithers & Parson, 1975). In general for a reaction to follow a second-order kinetics, there must be a bimolecular reaction that limits the rate even if the former reaction itself is first order. In our case the reaction could be second order if there is a protonation event that is the rate-limiting step for the electron transfer to occur. It is known that reduction of Q_A in the RC is connected to protonation events visible as a proton uptake. This was interpreted as a shift of the pK's of several amino acid residues in response to the charge transferred to the quinone (McPherson et al., 1988). The pK shifts will lead to the partial protonation of residues, i.e., at any time only a part of the residues will be protonated. If the protonation events occur on a functional time scale, this in turn could influence the electron transfer kinetics. Although not really resolved, we think that the complex reaction kinetics that is observed could be due to different energetic states of the acceptor site connected to partial rapid protonation.

We find that the first electron transfer to Q_B occurs with a half-time of about 20 μs and does not depend on pH. This half-time is in excellent agreement with that determined earlier by Carithers and Parson (1975) at pH >7.6 by measuring cytochrome oxidation on the second flash. Whereas the nonexponential form of their kinetics is also in accordance with our results, we could not confirm the strong acceleration upon lowering the pH. At present we cannot explain this discrepancy. The fact that we found the rate to be constant over a much wider pH range, however, lets a significant pH dependence below pH 8 in whole cells appear unlikely. Furthermore, the absolute rate as well as the pH dependence reported in this study are in agreement with recent results on chromatophores and RC of *Rps. viridis* obtained with two different optical methods (Mathis, personal communication).

The kinetics of the first electron transfer may be compared with data obtained in other purple bacteria. In *Rb. sphaeroides* this reaction was studied not only in the wild-type but in the recent years also in mutants with modified amino acid residues in the Q_B pocket. Early measurements showed a weak decrease of the rate of the first electron transfer by about a factor of 2 per pH unit (Wraight, 1979; Vermêglio, 1982). Kleinfeld et al. (1984) could not reproduce these results. Starting with about the same rate at pH 7 that corresponds to 200 μs, their rate starts to become proportional to the H^+ concentration above pH 9, very similar to the behavior found in this work for the second electron transfer in *Rps. viridis*. The slower rate at low pH in *Rb. sphaeroides* compared to *Rps. viridis* could well be a consequence of the different nature of Q_A. However, the different pH dependence is not easily understood if the high homology of this region is taken into account. Interestingly, in *Rb. sphaeroides* Glu-L212 was identified to be responsible for this pH dependence having an anomalously high pK of 9.5. In a mutant where Glu-L212 was changed for glutamine, the electron-transfer rate was completely independent of pH (Paddock et al., 1989). Because this residue is conserved in *Rps. viridis*, further studies on mutants of *Rps. viridis* will be necessary in order to understand the difference in the protonation events in *Rb. sphaeroides* and *Rps. viridis*.

Kinetics of the Second Electron Transfer, $Q_A^- \rightarrow Q_B^-$. When Q_B is in the semiquinone state the electron transfer between the quinones is decelerated. There is multiple evidence for this: the direct measurement of Q_A^- reoxidation after one, two, or three preflashes under conditions where Q_B was essentially oxidized before the preflash(es) (Figure 2), the mixing of faster and slower kinetics under conditions where Q_B was only partly oxidized before the preflash(es) (Figure 4), and the binary oscillation of the fraction of Q_A^- at a certain delay time after the last of a variable number of preflashes (Figure 3). The deceleration of the second electron transfer with respect to the first one becomes more pronounced with increasing pH especially above pH 9, where the rate decreases linearly with the bulk proton concentration (Figure 6).

There exist no data about the second electron transfer in *Rps. viridis*. But in *Rb. sphaeroides* as well as in photosystem II a similar deceleration of the second electron transfer compared to the first one was found (Wraight, 1979; Bowes & Crofts, 1980; Vermêglio, 1982; Kleinfeld et al. 1985). Qualitatively the pH dependence found in *Rb. sphaeroides* compares to our data: the second electron transfer shows a slight pH dependence at low pH and becomes roughly proportional to the H^+ concentration above pH 8.

The deceleration compared to the first electron transfer can be interpreted as the effect of the negative charge on Q_B^- that hinders the second electron transfer by coulombic repulsion. The strong pH dependence above pH 9 indicates that a protonation event controls the electron transfer. We did not observe a clear titration wave between a fast and a slow phase but rather a continuous decrease of a single rate. This suggests that it is not the static protonation state of a single residue

with a pK of about 9.4 that governs the kinetics. It is more likely that a proton has to be supplied directly to the quinone to stabilize the second electron. If the groups involved in the proton transfer chain to Q_B are strongly coupled, it is not necessarily the pK of the direct proton donor to Q_B that is observed but perhaps that of a secondary donor. Even more simply at high pH, the uptake of a proton from the bulk phase could be the rate-limiting step for electron transfer. This would explain the linear relationship between H^+ concentration and electron transfer rate. At lower pH the proton or electron transfer per se could be limiting. Although it seems obvious that the second electron transfer is strongly coupled to protonation of Q_B, the exact order of events, which depends on the redox chemistry of Q_B in vivo, still remains an open question (Wraight, 1982; Takahashi & Wraight, 1990).

Studies with mutants of *Rb. sphaeroides* where protonatable amino acid residues in the Q_B pocket have been replaced by unprotonatable ones allowed the identification of several residues that are involved in the proton transfer to Q_B and their effect on the electron transfer. It has been proposed that the first proton to Q_B, strongly coupled to the second electron transfer, comes via a hydrogen bond from Ser-L223, which again seems to be reprotonated by Asp-L213 (Paddock et al., 1990; Takahashi & Wraight, 1990). The second proton, which is involved in quinol formation, comes from Glu-L212 (Paddock et al., 1989). This residue, as already stated, is also responsible for the pH dependence of the first electron transfer in *Rb. sphaeroides*. The residues Ser-L223 and Glu-L212 are present also in *Rps. viridis* and for both there exist mutants (Sinning et al., 1989; Ewald et al., 1990). The study of the electron transfer in these mutants will help to further characterize the role of these conserved amino acid residues.

With this study we showed that time-resolved photovoltage measurements in the picosecond and nanosecond time range can successfully be used to study electron transfer between the primary and the secondary (quinone) acceptor in photosynthetic RC occurring on a much slower time scale. The method is based on a kinetic analysis of the electrogenic events of forward and backward reactions switched by the presence of an electron on Q_A. As a double-flash method, it is applicable to cases where the donation to the oxidized primary donor after a single-turnover flash is faster than the reoxidation kinetics of the acceptor under study. In mutants in which amino acid residues in the region of the quinone–iron acceptor complex are modified, Q_B or even Q_A are often not stable in isolated RC. The fact that photovoltage signals with a sufficient signal-to-noise ratio can be obtained from whole cells makes it a promising method for the study, in site-specific mutants, of the structure–function relationship of this reaction that links electron and proton transport in photosynthetic energy conversion.

Acknowledgments

We thank W. Nitschke, P. Sebban, A. Verméglio, H.-W. Trissl, and P. Mathis for useful discussions, A. W. Rutherford for many stimulating and helpful discussions, and W. Junge for critical comments. We also acknowledge P. Mathis for sharing his results prior to publication.

References

Baciou, L., Rivas, E., & Sebban, P. (1990) *Biochemistry 29*, 2966–2976.

Bowes, J. M., & Crofts, A. R. (1980) *Biochim. Biophys. Acta 590*, 373–384.

Carithers, R. P., & Parson, W. W. (1975) *Biochim. Biophys. Acta 387*, 194–211.

Cohen-Bazire, G., Sistrom, W. R., & Stanier, R. Y. (1957) *J. Cell. Comp. Physiol. 49*, 25–68.

Crofts, A. R., & Wraight, C. A. (1983) *Biochim. Biophys. Acta 726*, 149–185.

Deprez, J., Trissl, H.-W., & Breton, J. (1986) *Proc. Natl. Acad. Sci. U.S.A. 83*, 1699–1703.

Diner, B. A., Schenck, C. C., & De Vitry, C. (1984) *Biochim. Biophys. Acta 766*, 9–20.

Dobek, A., Deprez, J., Paillotin, G., Leibl, W., Trissl, H.-W., & Breton, J. (1990) *Biochim. Biophys. Acta 1015*, 313–321.

Dracheva, S. M., Drachev, L. A., Konstantinov, A. A., Semenov, A. Yu., Skulachev, V. P., Arutjunjan, A. M., Shuvalov, V. A., & Zaberezhnaya, S. M. (1988) *Eur. J. Biochem. 171*, 253–264.

Ewald, G., Wiessner, C., & Michel, H. (1990) *Z. Naturforsch. 45c*, 459–462.

Feher, G., Allen, J. P., Okamura, M. Y., & Rees, D. C. (1989) *Nature 339*, 111–116.

Gao, J.-L., Shopes, R. J., & Wraight, C. A. (1990) *Biochim. Biophys. Acta 1015*, 96–108.

Gao, J.-L., Shopes, R. J., & Wraight, C. A. (1991) *Biochim. Biophys. Acta 1056*, 259–272.

Holten, D., Windsor, M. W., Parson, W. W., & Thornber, J. P. (1978) *Biochim. Biophys. Acta 501*, 112–126.

Huber, R. (1989) *EMBO J. 8*, 2125–2147.

Kleinfeld, D., Okamura, M. Y., & Feher, G. (1984) *Biochim. Biophys. Acta 766*, 126–140.

Kleinfeld, D., Okamura, M. Y., & Feher, G. (1985) *Biochim. Biophys. Acta 809*, 291–310.

Leatherbarrow, R. J. (1989) *GraFit*, Erithacus Software Ltd., Staines, U.K.

Leibl, W., & Trissl, H.-W. (1990) *Biochim. Biophys. Acta 1015*, 304–312.

Maroti, P., & Wraight, C. A. (1988) *Biochim. Biophys. Acta 934*, 329–347.

McPherson, P. H., Okamura, M. Y., & Feher, G. (1988) *Biochim. Biophys. Acta 934*, 348–368.

McPherson, P. H., Okamura, M. Y., & Feher, G. (1990) *Biochim. Biophys. Acta 1016*, 289–292.

Mulkidjanyan, A. Ya., Shinkarev, V. P., Verkhovsky, M. I., & Kaurov, B. S. (1986) *Biochim. Biophys. Acta 849*. 150–161.

Paddock , M. L., Rongey, S. H., Feher, G., & Okamura, M. Y. (1989) *Proc. Natl. Acad. Sci. U.S.A. 86*, 6602–6606.

Paddock, M. L., McPherson, P. H., Feher, G., & Okamura, M. Y. (1990) *Proc. Natl. Acad. Sci. U.S.A. 87*, 6803–6807.

Parson, W. W. (1969) *Biochim. Biophys. Acta 189*, 384–396.

Prince, R. C., Leigh, J. S., & Dutton, P. L. (1976) *Biochim. Biophys. Acta 440*, 622–636.

Prince, R. C., Linkletter, S. J. G., & Dutton, P. L. (1981) *Biochim. Biophys. Acta 635*, 132–148.

Rutherford, A. W., & Evans, M. C. W. (1979) *FEBS Lett. 104*, 227–230.

Rutherford, A. W., Heathcote, P., & Evans, M. C. W. (1979) *Biochem. J. 182*, 515–523.

Sebban, P., & Barbet, J. C. (1984) *FEBS Lett. 165*, 107–110.

Shopes, R. J., & Wraight, C. A. (1985) *Biochim. Biophys. Acta 806*, 348–356.

Shopes, R. J., & Wraight, C. A. (1986) *Biochim. Biophys. Acta 848*, 364–371.

Sinning, I., Michel, H., Mathis, P., & Rutherford, A. W. (1989) *Biochemistry 28*, 5544–5553.

Takahashi, E., & Wraight, C. A. (1990) *Biochim. Biophys. Acta 1020*, 107–111.

Trissl, H.-W., Breton, J., Deprez, J., & Leibl, W. (1987a) *Biochim. Biophys. Acta 893*, 305–319.
Trissl, H.-W., Leibl, W., Deprez, J., Dobek, A., & Breton, J. (1987b) *Biochim. Biophys. Acta 893*, 320–332.
Trissl, H.-W., Breton, J., Deprez, J., Dobek, A., & Leibl, W. (1990) *Biochim. Biophys. Acta 1015*, 322–333.
Venturoli, G., & Zannoni, D. (1988) *Eur. J. Biochem. 178*, 503–509.
Verméglio, A. (1977) *Biochim. Biophys. Acta 459*, 516–524.
Verméglio, A. (1983) in *Function of Quinones in Energy Conserving Systems* (Trumpower, B. L., Ed.) pp 169–180, Academic Press, New York.
Verméglio, A., & Clayton, R. K. (1977) *Biochim. Biophys. Acta 461*, 159–165.
Verméglio, A., Martinet, T., & Clayton, R. K. (1980) *Proc. Natl. Acad. Sci. U.S.A. 77*, 1809–1813.
Woodbury, N. W. T., & Parson, W. W. (1984) *Biochim. Biophys. Acta 767*, 345–361.
Wraight, C. A. (1977) *Biochim. Biophys. Acta 459*, 525–531.
Wraight, C. A. (1979) *Biochim. Biophys. Acta 548*, 309–327.
Wraight, C. A. (1982) in *Function of Quinones in Energy Conserving Systems* (Trumpower, B. L., Ed.) pp 181–197, Academic Press, New York.
Wraight, C. A., Shopes, R. J., & McComb, J. C. (1987) in *Progress in Photosynthesis Research* (Biggins, J., Ed.) Vol. II, pp 387–396, Martinus Nijhoff, Dordrecht, The Netherlands.
Wraight, C. A., & Stein, R. R. (1980) *FEBS Lett. 113*, 73–77.

Biochemical and Kinetic Characteristics of the Interaction of the Antitumor Antibiotic Sparsomycin with Prokaryotic and Eukaryotic Ribosomes†

Ester Lazaro,‡ Leon A. G. M. van den Broek,§ Ana San Felix,‡ Harry C. J. Ottenheijm,§ and Juan P. G. Ballesta*,‡

Centro de Biologia Molecular, CSIC-UAM, Canto Blanco, 28049 Madrid, Spain, and Department of Organic Chemistry, University of Nijmegen, Toernooiveld, 6525 ED Nijmegen, The Netherlands

Received March 29, 1991; Revised Manuscript Received June 24, 1991

ABSTRACT: Using ^{125}I-labeled phenol–alanine sparsomycin, an analogue of sparsomycin having higher biological activity than the unmodified antibiotic, we studied the requirements and the characteristics of its interaction with the ribosome. The drug does not bind to either isolated ribosomal subunits or reconstituted whole ribosomes. For sparsomycin binding to 70S and 80S ribosomes, the occupation of the peptidyl-transferase P-site by an N-blocked aminoacyl-tRNA is a definitive requirement. The sparsomycin analogue binds to bacterial and yeast ribosomes with K_a values of around 10^6 M^{-1} and 0.6×10^6 M^{-1}, respectively, but its affinity is probably affected by the character of the peptidyl-tRNA bound to the P-site. Chloramphenicol, lincomycin, and 16-atom ring macrolides compete with sparsomycin for binding to bacterial ribosomes, but streptogramins and 14-atom ring macrolides do not. Considering the reported low affinity of puromycin for bacterial ribosomes, this antibiotic is also a surprisingly good competitor of sparsomycin binding to these particles. In the case of yeast ribosomes, blasticidin is a relatively good competitor of sparsomycin interaction, but anisomycin, trichodermin, and narciclasin are not. As expected, puromycin is a poor competitor of the binding in this case. The results from competition studies carried out with different sparsomycin analogues reveal, in some cases, a discrepancy between the drug ribosomal affinity and its biological effects. This suggests that some intermediate step, perhaps a ribosomal conformational change, is required for the inhibition to take place.

Sparsomycin[1] (Figure 1) is a broad-spectrum antibiotic that inhibits protein synthesis by interacting with the ribosome at the peptidyl transferase center, blocking peptide bond formation [see Ottenheijm et al. (1986) for a review on sparsomycin]. Lately, the preparation of sparsomycin derivatives considerably more active than the original drug (van den Broek et al., 1987, 1989)—some of which have produced promising results in ongoing clinical tests (Zylicz, 1988)—has stirred up new interest in this drug as an antitumor agent. Sparsomycin is also of considerable interest from an even more basic point of view since its strong inhibitory activity on all cell types, including the highly resistant archaebacteria (Cammarano et al., 1985), indicates the existance of a highly conserved target for drug action in all ribosomes. In fact, sparsomycin has been extensively used as a tool in ribosome and protein synthesis studies (Ottenheijm et al., 1986). The drug has been found to induce intriguing effects on the ribosomal particle, confirming a close interrelation between the A- and P-sites in the peptidyl transferase center. Thus, sparsomycin blocks the

† This work has been supported by grant PB87-0450 from the Dirección General de Politica Cientifica (Spain), by an institutional grant to the Centro de Biologia Molecular from the Fundacion Ramon Areces (Madrid), and by a grant from the Netherlands Foundation for Chemical Research (SON) with financial aid from the Netherlands Organization for Scientific Research (NWO).

‡ Centro de Biologia Molecular, CSIC-UAM.
§ University of Nijmegen.

[1] Abbreviations: sparsomycin, *N*-[1-(hydroxymethyl)-2-[[(methylthio)methyl]sulfinyl]ethyl]-3-(1,2,3,4-tetrahydro-6-methyl-2,4-dioxo-5-pyrimidinyl)-2-propenamide; phenol–alanine sparsomycin, derivative in which the (methylthio)methyl group has been replaced by 4-hydroxyphenyl and the hydroxymethyl group has been replaced by methyl, i.e., *N*-[1-methyl-2-[(4-hydroxyphenyl)sulfinyl]ethyl]-3-(1,2,3,4-tetrahydro-6-methyl-2,4-dioxo-5-pyrimidinyl)-2-propenamide.

0006-2960/91/0430-9642$02.50/0